Genes to Cells

Neural crest-derived multipotent cells in the adult mouse iris stroma

Miki Kikuchi[1], Ryuhei Hayashi[1], Sachiko Kanakubo[1,2], Ayumi Ogasawara[2], Masayuki Yamato[3], Noriko Osumi[2] and Kohji Nishida[1]*

[1]*Department of Ophthalmology, Tohoku University School of Medicine, Sendai, Japan*
[2]*Division of Developmental Neuroscience, Center for Translational and Advanced Animal Research, Tohoku University School of Medicine, 1-1 Seiryomachi, Aoba-ku, Sendai 980-8574, Japan*
[3]*Institute of Advanced Biomedical Engineering and Science, Tokyo Women's Medical University, Tokyo, Japan*

The purpose of this study was to characterize neural crest–derived cells within the adult murine iris. The iris was isolated from P0-Cre/Floxed-EGFP transgenic (TG) mice. The isolated iris cells formed EGFP-positive spheres on non-adhesive culture plates. Immunostaining showed that these EGFP-positive spheres expressed neural crest markers including Sox10 and p75NTR, and these cells showing *in vitro* sphere-forming ability were originally resided in the iris stroma (IS), *in vivo*. Real-time RT-PCR showed that the EGFP-positive spheres expressed significantly higher levels of the neural crest markers than EGFP-negative spheres and bone marrow–derived mesenchymal stem cells. Furthermore, the iris stromal sphere had capability to differentiate into various cell lineages including smooth muscle and cartilage. These data indicate that neural crest–derived multipotent cells can be isolated from the murine IS and expanded in sphere culture.

Introduction

During development, the neural crest generates various cell types in adult vertebrate organisms, including cells that give rise to the autonomic nervous system, primary sensory neurons, smooth muscle of the cardiac outflow tract, melanocytes, cranial mesenchymal tissues, and some ocular tissues (Osumi-Yamashita *et al.* 1994; Le Douarin & Kalcheim 1999). Recent reports have showed that in adult tissues, neural crest–derived tissue-specific stem/progenitor cells are widely distributed, as they were observed in the skin, cardiac muscle, and corneal stroma (CS) (Toma *et al.* 2001; Tomita *et al.* 2005; Wang *et al.* 2006; Yoshida *et al.* 2006; Yu *et al.* 2006). These neural crest–derived cells have the capability to differentiate into multiple cell lineages originating from the neural crest. Therefore, these cells are thought to be 'neural crest stem cells' (Morrison *et al.* 1999; Dupin *et al.* 2007).

Previous embryonic developmental analyses using TG mouse and chicken embryos suggest that many of the ocular tissues originate from the cranial neural crest (Gage *et al.* 2005). Cranial neural crest–derived anterior segments of the eye are thought to develop in the following three steps (Saika *et al.* 2001; Jin *et al.* 2002). The first wave of neural crest cells differentiates to form the trabecular meshwork (TM) and corneal endothelium (CEnd). The second wave gives rise to CS cells, and the third wave contributes to the development of the iris. Among eye tissues that are from neural crest-originated cells, the iris is the only tissue that can be isolated by routine ophthalmological surgery. The iris therefore could be an excellent cell source for regenerative therapy of neural crest–originated ocular tissues. In this study, we report the isolation and characterization of neural crest–derived cells in the adult murine iris stroma (IS).

Results

Localization of cells derived from the neural crest in the anterior segment of the mouse eye

P0-Cre; EGFP mice were generated by crossing TG mice expressing Cre enzyme driven by the P0 promoter with *CAG-CAT-EGFP* TG line (Fig. 1A).

Communicated by: Masayuki Yamamoto (Tohoku University)
**Correspondence:* knishida@oph.med.tohoku.ac.jp

DOI: 10.1111/j.1365-2443.2011.01485.x

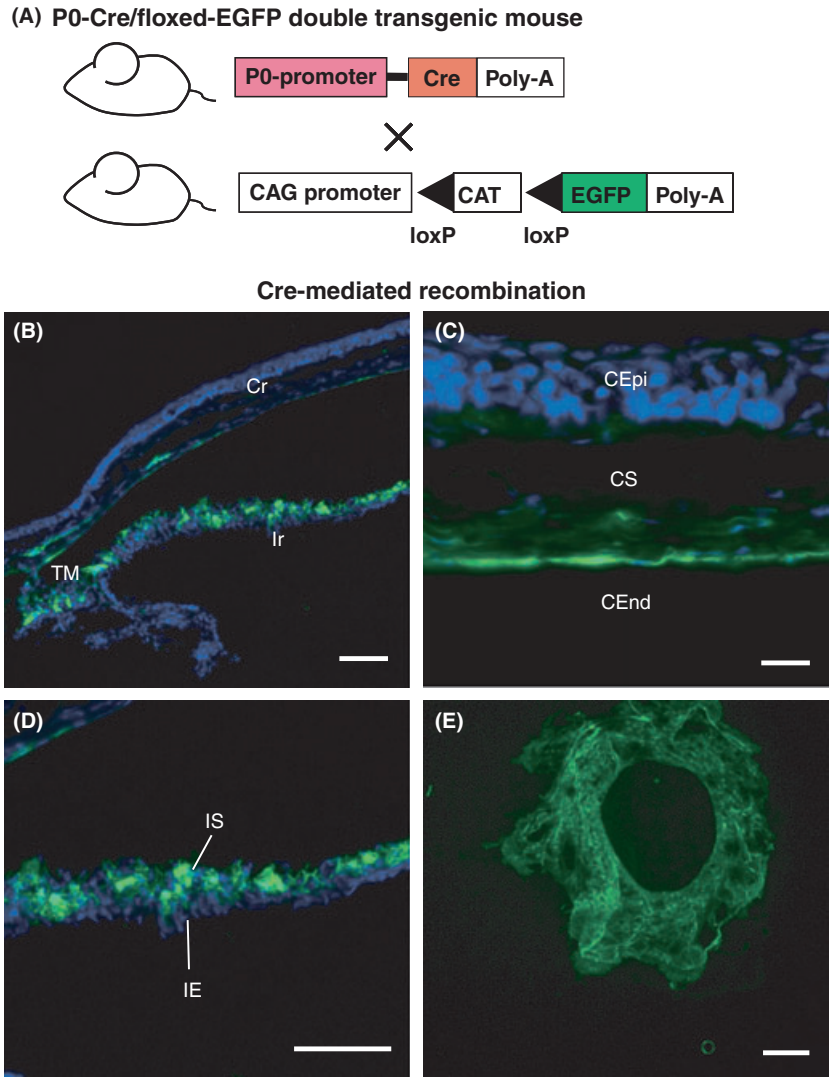

Figure 1 Distribution of EGFP-positive cells in the anterior segment of the P0-Cre; EGFP mouse eye. Transgenic (TG) mice expressing the Cre enzyme driven by the myelin protein zero (P0) promoter were crossed with the TG line, *CAG-CAT-EGFP* (A). EGFP-labeled cells (green) were observed in the iris (Ir), trabecular meshwork and cornea (Cr) (B). Magnified view of (B) shows EGFP-positive cells localized in the corneal endothelium, part of the corneal stroma and the iris stroma (C–D). Isolated iris tissue was observed by fluorescent microscopy (E). IE, Iris pigment epithelium; CEpi, corneal epithelium. Scale bar: 100 μm (B, D), 20 μm (C), 400 μm (E).

Immunofluorescence staining showed that EGFP was expressed in the iris (Ir), TM, and cornea (Cr) (Fig. 1B). A magnified view of Fig. 1B shows that EGFP-positive cells were specifically localized in the CEnd, as well as part of the CS and the IS (Fig. 1C–D). EGFP expression was also observed in the whole area of irises enucleated from the eyes of P0-Cre; EGFP mice (Fig. 1E). These expression patterns confirmed data in the previous reports (Kanakubo *et al.* 2006; Yoshida *et al.* 2006).

In vivo localization of Sox10 and p75NTR positive cells in the iris tissue of P0-Cre; EGFP mice

The expressions of Sox10 and p75NTR, typical neural crest markers, were examined in the iris tissue by Immunostaining. The result showed that both Sox10 and p75NTR were localized only in the iris stromal part (Fig. 2A–F). These neural crest markers were co-expressed with EGFP in the most part of iris stromal cells. The Immunofluorescent staining of

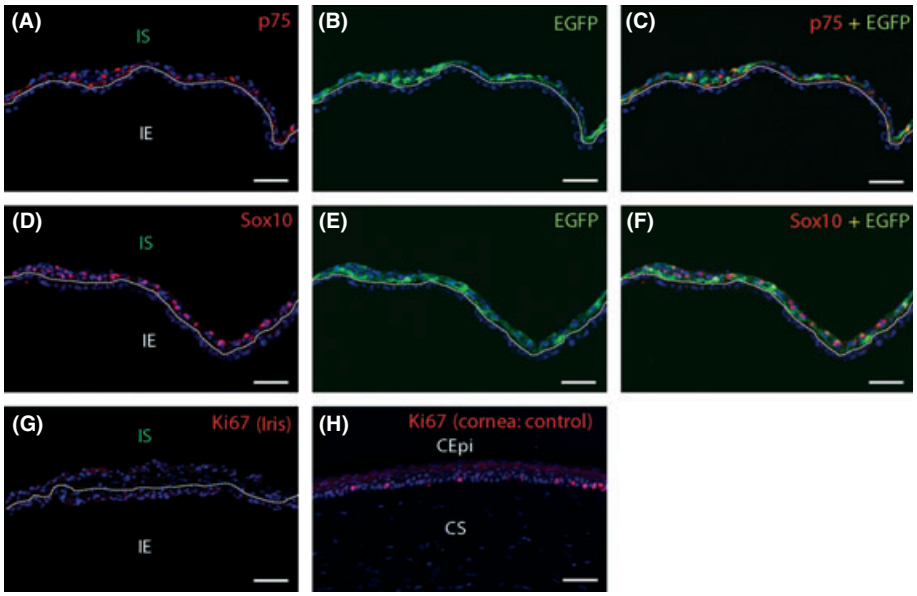

Figure 2 *In vivo* localization of neural crest and proliferation markers in the iris of P0-Cre; EGFP mouse. The expressions of sox10 and p75NTR, typical neural crest markers, in the iris tissue were examined by immunostaining. Both p75NTR (A–C) and sox10 (D–F) were localized only in the iris stromal part. These neural crest markers were co-expressed with EGFP in the large part of iris stromal cells. The immunostaining of Ki67 showed that there was no Ki67-positive proliferating iris cell *in vivo* (G). Control slide showed that Ki-67 positive cells in existed in the basal layer of corneal epithelium (H). Scale bar: 50 μm.

a proliferation marker Ki67 indicated that there were almost no proliferating cells in the normal iris tissue *in vivo*. (Fig. 2G). Therefore, EGFP-positive neural crest–derived cells seem to be non-proliferative in the normal homeostatic condition.

Sphere formation from iris cells of P0-Cre; EGFP mice

To characterize the EGFP-positive cells in the iris, we performed sphere formation assays. Iris cells isolated from P0-Cre; EGFP mice were cultured in non-adhesive culture plates. A number of EGFP-positive spheres were formed from the iris cells (Fig. 3A). Some of the EGFP-positive iris cells dissociated from the primary spheres had a capability to form secondary spheres (Fig. 3B). Supporting a previous report (Yoshida *et al.* 2006), it thus suggested that there are stem cell-like cells that can be grown in sphere culture in the iris cells.

Immunostaining of stem cell and neural crest markers

Immunostaining showed that the spheres were composed of EGFP-positive iris stromal cells and expressed stem cell markers such as Nestin and Sox2 (Fig. 3C–E). They also expressed typical neural crest markers, such as Sox10, p75NTR, and AP-2β (Fig. 3F–H) (Kanakubo *et al.* 2006; Lee *et al.* 2007). Furthermore, BrdU assay showed that BrdU- and Ki67-positive cells existed in the iris spheres (Fig. 3I–J). This means that the sphere culture condition has successfully turned EGFP-positive dormant neural crest–derived cells into proliferative.

Fluorescence activated cell sorting and gene expression analyses of stem cell and neural crest markers

Flow cytometric analysis showed that iris cells consisted of $39.8 \pm 2.3\%$ ($N = 6$) EGFP-positive iris stromal cells (Fig. 4A). Sphere culture showed that both isolated EGFP-positive and EGFP-negative cells could form spheres after 5 days of culture (Fig. 4B), and their sphere-forming efficiencies were $0.60 \pm 0.079\%$ and $0.46 \pm 0.053\%$, respectively ($N = 5$). The harvested EGFP-positive iris stromal spheres expressed the stem cell markers Sox2, Nestin and Musashi1 as well as the neural crest makers Slug, p75NTR, Sox9, 10, AP-2α and β (Fig. 4C). Real-time RT-PCR showed that the EGFP-positive

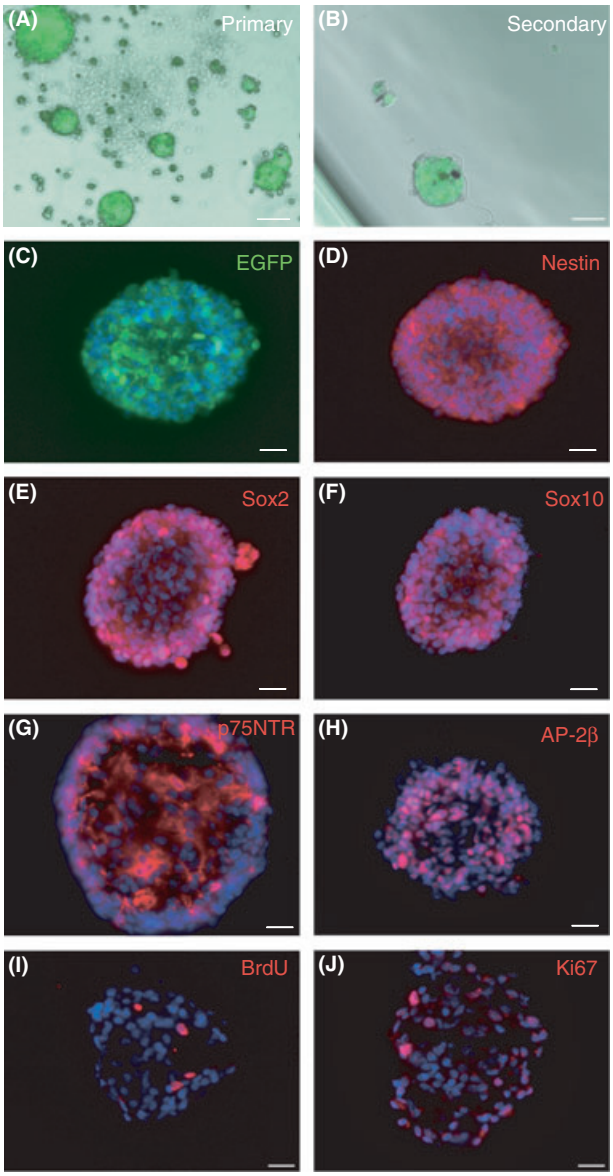

Figure 3 Sphere culture and immunofluorescence staining of stem cell- and neural crest–related markers. Cells were isolated from iris tissue and then cultured in non-adhesive culture plates to form spheres. Microscopic observation showed that EGFP-positive spheres formed after 7 days of culture (A). A subset of EGFP-positive cells from primary spheres formed secondary spheres (B). Observation of frozen sections showed that almost all of the cells that composed the spheres were EGFP positive (C; green). Immunofluorescence staining showed that cells in EGFP-positive iris spheres expressed the stem cell markers Nestin and Sox2 (D–E; red), as well as the neural crest markers Sox10, p75NTR, and AP-2β (F–H; red). In addition, BrdU- and Ki67-positive proliferating cells existed in iris spheres (I–J; red). Nuclei were labeled with Hoechst 33342 (blue). Scale bar: 100 μm (A, B), 20 μm (C–J).

spheres expressed significantly higher levels of the neural crest markers Sox10, p75NTR, and AP-2β than EGFP-negative spheres or bone marrow–derived mesenchymal stem cells (MSCs) (Fig. 4D).

Cell differentiation

To investigate the multipotency of the EGFP-positive iris stromal spheres, we performed differentiation assays for multiple neural crest cell lineages. EGFP-expressing cells migrated from the circumference of the spheres and co-expressed βIII-tubulin (11.5 ± 2.0%, $N = 8$), glial fibrillary acidic protein (GFAP) (28.8 ± 9.6%, $N = 4$) and alpha smooth muscle actin (αSMA) (74.0 ± 9.6%, $N = 4$) (Fig. 5A–F). Pellet cultures showed that most of the aggregated cells were stained with alcian blue and also expressed aggrecan and type II collagen (Fig. 5G–I), typical differentiation markers of chondrocytes. Statistical analyses of the differentiation efficiencies were shown in Table 1. These data suggest that EGFP-positive cells have potentials to differentiate into various cell types in cultures.

Discussion

Our observation of the anterior segment of the P0-Cre; EGFP mouse eye showed EGFP-positive cells in the CEnd, TM, and IS. In contrast, there was no EGFP-positive cell in iris pigment epithelium and corneal epithelium that were generated from neural and surface ectoderm. These data support the previous reports that the P0-Cre; EGFP mouse allows accurate labeling of neural crest–derived tissues (Jin *et al.* 2002; Kanakubo *et al.* 2006; Yoshida *et al.* 2006). EGFP-positive cells isolated from the iris could form EGFP-positive spheres on non-adhesive culture plates. Secondary sphere culture showed that at least some iris stromal cells in the primary EGFP-positive iris spheres had the ability to reform spheres. Additionally, BrdU assay and Ki67 staining showed that a subgroup of BrdU- and Ki67-positive proliferating cells existed in the primary spheres, although there were no proliferating cells in the iris tissue *in vivo*. These findings suggest that the iris spheres are formed as a result of proliferation of the iris cells, rather than by aggregation.

Immunostaining of spheres for stem cell markers showed that EGFP-positive iris spheres expressed not only the stem cell markers generally expressed in various tissue-specific stem cells, i.e. Nestin, Musashi1, and Sox2, but also typical neural crest markers such as

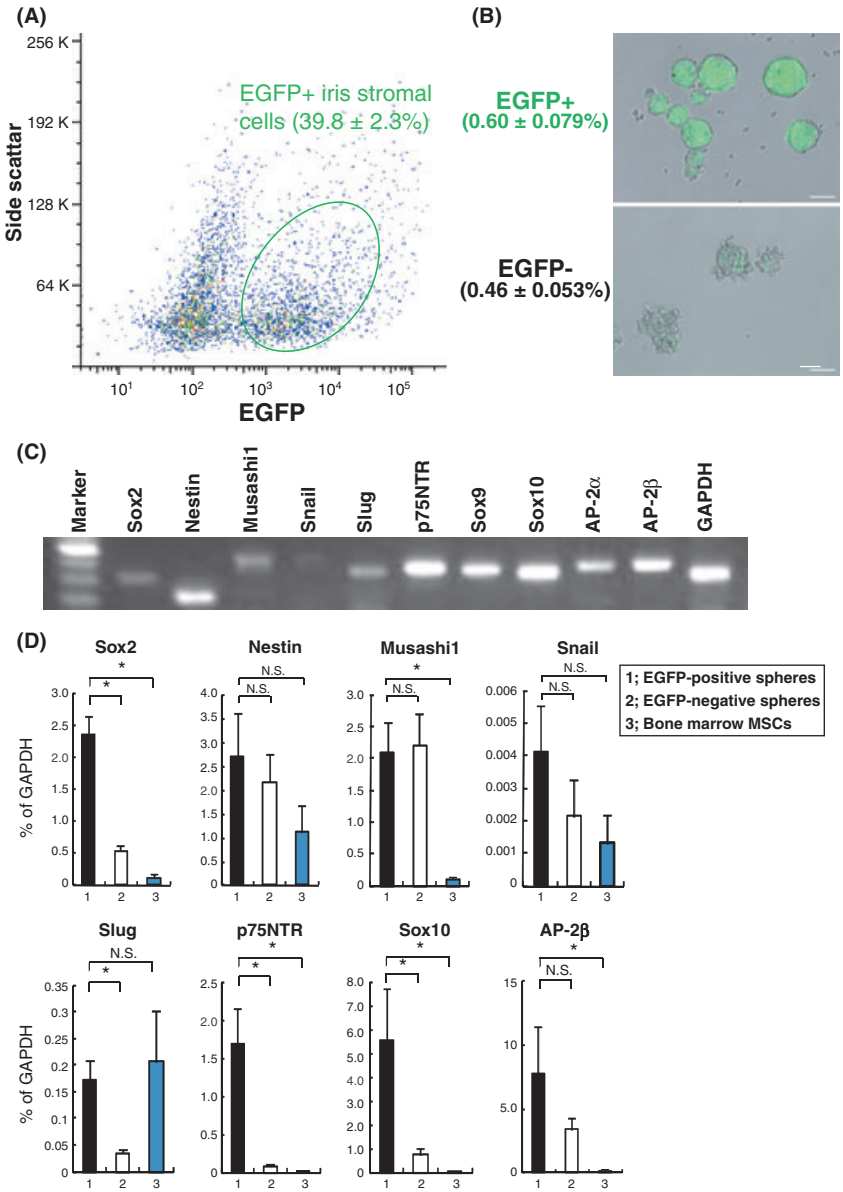

Figure 4 FACS and gene expression analyses of stem cell and neural crest–related markers in iris stromal spheres. Isolated iris cells from P0-Cre; EGFP mice were submitted to FACS (A). The iris cells were composed of approximately 39.8 ± 2.3% (mean ± SE, $N = 6$) EGFP-positive cells. After 5 days of sphere culture, the isolated EGFP-positive and EGFP-negative cells formed each sphere (B). And their sphere-forming efficiencies were 0.60 ± 0.079% and 0.46 ± 0.053%, respectively (mean ± SE, $N = 5$). RT-PCR showed that the EGFP-positive spheres expressed the stem cell markers Nestin, Musashi1, and Sox2, as well as the neural crest markers Slug, p75NTR, Sox9, Sox10, and AP-2α and AP-2β (C). Real-time RT-PCR showed that the EGFP-positive spheres expressed significantly higher levels of neural crest marker genes, Sox10, p75NTR, and AP-2β than EGFP-negative spheres or mesenchymal stem cells (D). Scale bar: 50 μm. The graphs show the mean ± SE of 4–6 independent samples. *indicates $P < 0.05$.

p75NTR, AP-2β, and Sox10 (Morrison *et al.* 2000; Lee *et al.* 2007). Some of these markers, including Sox2 and Sox10, seemed to be expressed more strongly in the peripheral part of the spheres than in the central part. As it was previously reported, the differentiation status may be different between peripheral and central parts of the spheres (Campos 2004).

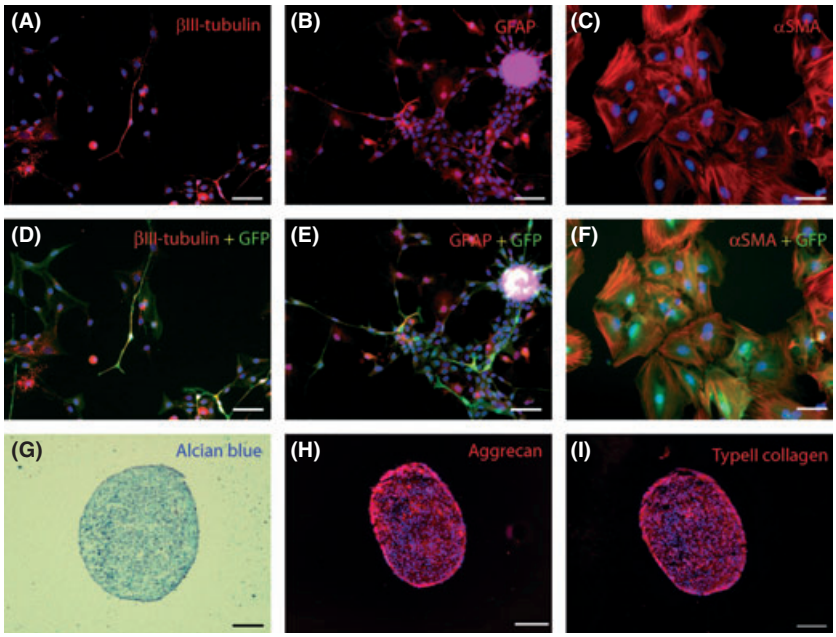

Figure 5 Multipotency of the iris stromal spheres. EGFP-positive iris stromal cells differentiated into neurons [A; βIII-tubulin (red), D; βIII-tubulin + EGFP (green) merge], glia [B; glial fibrillary acidic protein (GFAP) (red), E; GFAP + EGFP (green) merge] and smooth muscle cells [C; alpha smooth muscle actin (αSMA) (red), F; αSMA + EGFP (green) merge]. Pellet culture induced the differentiation of EGFP-positive iris cells into chondrocytes [G; Alcian blue, H; Aggecan (red), I; TypeII collagen (red)]. Nuclei were labeled with Hoechst 33342 (blue). Scale bar: 50 μm (A–F), 100 μm (G–I).

Table 1 Differentiation efficiencies of the iris stromal spheres

	βIII tublin+	Glial fibrillary acidic protein+	Alpha smooth muscle actin+
Differentiation efficiency ± SE (%)	11.5 ± 2.0 (N = 8)	28.8 ± 9.6 (N = 4)	74.0 ± 9.6 (N = 4)

Differentiation efficiencies to each cell lineage from the iris stromal spheres are expressed as means ± SE of 4–8 independent samples.

In vivo immunostaining for Sox10, p75NTR, and Ki67 suggested that these neural crest–derived cells showing *in vitro* sphere-forming abilities were originally retained in the IS on a quiescent state. On the other hand, there seemed to be some EGFP-negative cells existing in iris stromal part although it was difficult to confirm the co-expression of EGFP, Sox10, and p75NTR because of the differential expression, in cytoplasm, nuclei and on cell surface, respectively. To verify the neural crest–derived cells in adult tissue, it may be better to use other TG mice such as Wnt-1-Cre; EGFP mice in addition to P0-Cre; EGFP mice (Chai *et al.* 2000). At the same time, it can be thought that if the cells are EGFP-positive in P0-Cre; EGFP mice, they are surely originated from neural crest.

From FACS analysis, we showed that the iris tissue consists of 39.8% EGFP-positive cells comprising iris stromal cells, and EGFP-negative cells, a large part of which were thought to be iris pigment epithelial cells. Although both EGFP-positive and EGFP-negative iris cells formed spheres, quantitative RT-PCR showed EGFP-positive spheres expressed significantly higher levels of neural crest markers such as Slug, Sox10 and p75NTR than EGFP-negative spheres. These data indicated that although both IS and iris epithelium contained cells with stem/progenitor cell like property, the nature of each cell may be different.

Furthermore, differentiation assays showed that the EGFP-positive spheres had the ability to differentiate into neurons, glia, chondrocytes, and smooth muscle cells, all of which are generated from the cranial neural crest in normal development. In the current culture conditions, they seemed to have high differentiation capability to smooth muscle cells and chon-

drocytes. Although we investigated differentiation into melanocytes, which is of trunk neural crest origin (Erickson & Goins 1995), only few melanocytic differentiations were observed (data not shown). Previous report showed that neural crest–derived multipotent cells from skin could differentiate into melanocytes (Wang *et al.* 2006). These findings may reflect differential characters of the crest cells between trunk (melanocyte) and cranial (IS) origins.

In particular, eye has a lot of tissues which are derived from neural crest. Among these tissues, corneal endothelial cells and stromal cells are more important for regenerative medicine, because both CEnd and stroma has almost no regenerative capacity *in vivo*. Corneal endothelial or stromal cells were migrated from 'periocular mesenchyme' in a developmental stage in the same way as iris stromal cells (Saika *et al.* 2001; Jin *et al.* 2002). So cell lineages of these tissues are thought to be developmentally close. Furthermore, the iris can be safely isolated by routine ophthalmologic surgery. These facts suggested that the multipotent neural crest–derived cells in IS have great potential as a cell source for the regenerative medicine of damaged these corneal tissues.

Taking altogether, we showed that 'neural crest–derived multipotent cells' are specifically retained in the adult iris stromal part and can be isolated in sphere culture. To the best of our knowledge, this is the first report to isolate neural crest–derived cells with multipotency from the adult mice iris.

Experimental procedures

Animals

Transgenic mice expressing the Cre enzyme driven by the myelin protein zero (P0) promoter were crossed with the *CAG-CAT-EGFP* TG line (Yamauchi *et al.* 1999). In P0-Cre/floxed-EGFP double TG (P0-Cre; EGFP) mice, neural crest–derived cells were identified by evaluating EGFP expression after P0-Cre-mediated DNA recombination (Iwao *et al.* 2008). To eliminate pigmentation in the iris tissue of the double TG lines, these mice, originally of C57/BL6J background, were crossed with mice of an ICR background (Japan Charles River, Tokyo, Japan) for 5–6 generations. The P0-Cre recombinase TG mice were kindly provided by Dr K. Yamamura (Kumamoto University, Kumamoto, Japan). The *CAG-CAT-EGFP* TG mice were kindly provided by Dr J. Miyazaki (Osaka University, Osaka, Japan). All experimental procedures described in this study were approved by the Ethics Committee for Animal Experiments of Tohoku University Graduate School of Medicine.

Table 2 List of primers used for RT-PCR with corresponding amplicon sizes

Gene		Primer sequence (5′–3′)	Product size (bp)
Sox2	Forward	CCGTTTTCGTGGTCTTGTTT	313
	Reverse	ATACATGGATTCTCGGCAGC	
Nestin	Forward	AACTGCCCTAGAGACGGTGTCT	206
	Reverse	TCCCATTCACTTGCTCTGACTC	
Musashi1	Forward	GAGTTACACAGGCCTTGCCC	413
	Reverse	CCTCCTCCCTGTTTCAGTGG	
Snail	Forward	GAGGACAGTGGCAAAAGCTC	423
	Reverse	CTTCACATCCGAGTGGGTTT	
Slug	Forward	GCACTGTGATGCCCAGTCTA	347
	Reverse	AGCAGCCAGACTCCTCATGT	
p75NTR	Forward	CTGCTGCTTCTAGGGGTGTC	359
	Reverse	GAGAACACGAGTCCTGAGCC	
Sox9	Forward	AGCTCACCAGACCCTGAGAA	368
	Reverse	GATTCTCCAATCGTCCTCCA	
Sox10	Forward	GACTGAGCTGGCAAAGGAAG	332
	Reverse	GCGGAGAAAGGATCAGAGTG	
AP-2α	Forward	GCTGGGCACTGTAGGTCAAT	372
	Reverse	TGAGGTAAGGAGTGGATCGG	
AP-2β	Forward	CAGACGTGACAGCACCTGTT	393
	Reverse	TAGCAAGAAATCCAAAGCCG	
GAPDH	Forward	CCCACTAACATCAAATGGGG	324
	Reverse	ATCCACAGTCTTCTGGGTGG	

Cell culture

Iris were enucleated from adult P0-Cre; EGFP mice (4–8 weeks) and digested in Dulbecco's modified eagle medium (DMEM) containing collagenase (Sigma-Aldrich, St Louis, MO, USA), trypsin (Nacalai tesque, Kyoto, Japan) and DNase I (Sigma-Aldrich) for 20 min at 37 °C. Isolated iris cells were cultured in DMEM/F-12 (1 : 1), supplemented with 20 ng/mL epidermal growth factor (EGF; Sigma-Aldrich), 20 ng/mL basic fibroblast growth factor (bFGF; Invitrogen, Carlsbad, NM, USA), B27 supplement (Invitrogen) and 10^3 U/mL leukemia inhibitory factor (LIF; Chemicon International, Temecula, CA, USA) at 37 °C, 5% CO_2. The cells were seeded onto non-adhesive 96-well culture plates (CellSeed, Tokyo, Japan) and cultured for 5–7 days. To obtain secondary spheres, primary iris spheres were dissociated with 0.05% trypsin/0.53 mM EDTA-4Na (Invitrogen) into a single-cell suspension and then re-seeded into fresh medium. Mouse MSCs were prepared from bone marrow according to previous report (Tsuchiya *et al*. 2003).

Immunohistochemistry

Cultured cells and frozen tissue sections were fixed with 4% paraformaldehyde and then stained with the following primary antibodies: anti-Nestin (G-20; Santa Cruz Biotechnology, CA, USA), anti-Sox2 (Y-17; Santa Cruz Biotechnology), anti-Sox10 (N-20; Santa Cruz Biotechnology), anti-Ki67 (Abcam, Cambridge, UK), anti-alpha smooth muscle actin (αSMA; Abcam), anti-p75NTR (Abcam), anti-AP-2β (Cell Signaling Technology, Danvers, MA, USA), anti-βIII-tubulin (Tuj-1; R&D Systems, Minneapolis, MN, USA), anti-collagen type II (Chemicon), anti-aggrecan (Chemicon), anti-glial fibrillary acidic protein (GFAP; Chemicon) and anti-GFP antibody (MBL, Nagoya, Japan). After washing with Tris-buffered saline, the slides were stained with Alexa Fluor-488 or Alexa Fluor-568 conjugated secondary antibodies (Invitrogen). All sections were counterstained with Hoechst 33342 (Invitrogen).

Flow cytometric analysis and cell sorting

For flow cytometry and cell sorting, a FACSAria (BD Biosciences, San Diego, CA, USA) was used. Sorted EGFP-positive and EGFP-negative cells were resuspended in sphere culture medium and cultured in non-adhesive 96-well culture plates.

Reverse transcription-polymerase chain reaction

Total RNA was obtained from harvested EGFP-positive, EGFP-negative spheres and MSCs using the RNeasy total RNA micro kit (Qiagen, Valencia, CA, USA). Reverse transcription was performed with the SuperScript First-Strand Synthesis System for RT-PCR (Invitrogen), according to the manufacturer's suggested protocol. The RT-PCR thermocycle program consisted of an initial cycle at 94 °C for 5 min and 33 cycles at 94 °C for 30 s, 60 °C for 30 s and 72 °C for 30 s (PCR Thermal Cycler MP; Takara Bio, Shiga, Japan). Primer pairs are shown in Table 2. Quantitative real-time RT-PCR was performed using the ABI Prism 7900HT Sequence Detection System (Applied Biosystems Inc., Foster City, CA, USA), according to the manufacturer's suggested protocol. Primer pairs and TaqMan® MGB probes were designed with Assay-by-Design™ (Applied Biosystems).

Differentiation culture

To induce neurogenic and glial differentiation, EGFP-positive iris spheres were cultured in the sphere culture medium without bFGF, EGF, or LIF for 7 days on dishes coated with ornithine and laminin. For chondrogenic differentiation, the spheres were cultured with hMSC Differentiation Bulletkit, Chondrogenic (Takara Bio) according to the manufacturer's protocol. Chondrogenic differentiation was observed by evaluation of the expression of type II collagen and aggrecan (Chemicon International), and staining with alcian blue (Diagnostic Biosystems, Pleasanton, CA, USA). Smooth muscle differentiation was induced in DMEM/F12 containing 2% FBS and 10 ng/mL TGFβ1 (R&D Systems) for 7 days.

Statistical analysis

Data are expressed as means ± SE. Statistical analysis was performed using the Mann–Whitney rank sum test, and statistics were calculated using SigmaStat 3.5 (SPSS, Chicago, IL, USA).

Acknowledgements

This work was supported in part by Grants-in-Aid for Scientific Research from the Ministry of Health, Labor and Welfare and from National Institute of Biomedical Innovation in Japan.

References

Campos, L.S. (2004) Neurospheres: insights into neural stem cell biology. *J. Neurosci. Res.* **78**, 761–769.

Chai, Y., Jiang, X., Ito, Y., Bringas, P. Jr, Han, J., Rowitch, D.H., Soriano, P., McMahon, A.P. & Sucov, H.M. (2000) Fate of the mammalian cranial neural crest during tooth and mandibular morphogenesis. *Development* **127**, 1671–1679.

Dupin, E., Calloni, G., Real, C., Goncalves-Trentin, A. & Le Douarin, N.M. (2007) Neural crest progenitors and stem cells. *C. R. Biol.* **330**, 521–529.

Erickson, C.A. & Goins, T.L. (1995) Avian neural crest cells can migrate in the dorsolateral path only if they are specified as melanocytes. *Development* **121**, 915–924.

Gage, P.J., Rhoades, W., Prucka, S.K. & Hjalt, T. (2005) Fate maps of neural crest and mesoderm in the mammalian eye. *Invest. Ophthalmol. Vis. Sci.* **46**, 4200–4208.

Iwao, K., Inatani, M., Okinami, S. & Tanihara, H. (2008) Fate mapping of neural crest cells during eye development using a protein 0 promoter-driven transgenic technique. *Graefes Arch. Clin. Exp. Ophthalmol.* **246**, 1117–1122.

Jin, E.J., Burrus, L.W. & Erickson, C.A. (2002) The expression patterns of Wnts and their antagonists during avian eye development. *Mech. Dev.* **116**, 173–176.

Kanakubo, S., Nomura, T., Yamamura, K., Miyazaki, J., Tamai, M. & Osumi, N. (2006) Abnormal migration and distribution of neural crest cells in Pax6 heterozygous mutant eye, a model for human eye diseases. *Genes Cells* **11**, 919–933.

Le Douarin, N.M. & Kalcheim, C. (1999) *The Neural Crest*. Cambridge, UK: Cambridge University Press.

Lee, G., Kim, H., Elkabetz, Y., Al Shamy, G., Panagiotakos, G., Barberi, T., Tabar, V. & Studer, L. (2007) Isolation and directed differentiation of neural crest stem cells derived from human embryonic stem cells. *Nat. Biotechnol.* **25**, 1468–1475.

Morrison, S.J., Csete, M., Groves, A.K., Melega, W., Wold, B. & Anderson, D.J. (2000) Culture in reduced levels of oxygen promotes clonogenic sympathoadrenal differentiation by isolated neural crest stem cells. *J. Neurosci.* **20**, 7370–7376.

Morrison, S.J., White, P.M., Zock, C. & Anderson, D.J. (1999) Prospective identification, isolation by flow cytometry, and *in vivo* self-renewal of multipotent mammalian neural crest stem cells. *Cell* **96**, 737–749.

Osumi-Yamashita, N., Ninomiya, Y., Doi, H. & Eto, K. (1994) The contribution of both forebrain and midbrain crest cells to the mesenchyme in the frontonasal mass of mouse embryos. *Dev. Biol.* **164**, 409–419.

Saika, S., Liu, C.Y., Azhar, M., Sanford, L.P., Doetschman, T., Gendron, R.L., Kao, C.W. & Kao, W.W. (2001) TGFbeta2 in corneal morphogenesis during mouse embryonic development. *Dev. Biol.* **240**, 419–432.

Toma, J.G., Akhavan, M., Fernandes, K.J., Barnabe-Heider, F., Sadikot, A., Kaplan, D.R. & Miller, F.D. (2001) Isolation of multipotent adult stem cells from the dermis of mammalian skin. *Nat. Cell Biol.* **3**, 778–784.

Tomita, Y., Matsumura, K., Wakamatsu, Y., Matsuzaki, Y., Shibuya, I., Kawaguchi, H., Ieda, M., Kanakubo, S., Shimazaki, T., Ogawa, S., Osumi, N., Okano, H. & Fukuda, K. (2005) Cardiac neural crest cells contribute to the dormant multipotent stem cell in the mammalian heart. *J. Cell Biol.* **170**, 1135–1146.

Tsuchiya, H., Kitoh, H., Sugiura, F. & Ishiguro, N. (2003) Chondrogenesis enhanced by overexpression of sox9 gene in mouse bone marrow-derived mesenchymal stem cells. *Biochem. Biophys. Res. Commun.* **301**, 338–343.

Wang, C.E., Paratore, C., Dours-Zimmermann, M.T., Rochat, A., Pietri, T., Suter, U., Zimmermann, D.R., Dufour, S., Thiery, J.P., Meijer, D., Beermann, F., Barrandon, Y. & Sommer, L. (2006) Neural crest-derived cells with stem cell features can be traced back to multiple lineages in the adult skin. *J. Cell Biol.* **175**, 1005–1015.

Yamauchi, Y., Abe, K., Mantani, A., Hitoshi, Y., Suzuki, M., Osuzu, F., Kuratani, S. & Yamamura, K. (1999) A novel transgenic technique that allows specific marking of the neural crest cell lineage in mice. *Dev. Biol.* **212**, 191–203.

Yoshida, S., Shimmura, S., Nagoshi, N., Fukuda, K., Matsuzaki, Y., Okano, H. & Tsubota, K. (2006) Isolation of multipotent neural crest-derived stem cells from the adult mouse cornea. *Stem Cells* **24**, 2714–2722.

Yu, H., Fang, D., Kumar, S.M., Li, L., Nguyen, T.K., Acs, G., Herlyn, M. & Xu, X. (2006) Isolation of a novel population of multipotent adult stem cells from human hair follicles. *Am. J. Pathol.* **168**, 1879–1888.

Received: 12 July 2010
Accepted: 29 November 2010